Dynamical Signatures

Lyle Noakes
Alistair Mees

SFI WORKING PAPER: 1991-09-038

SANTA FE INSTITUTE

Dynamical Signatures

Lyle Noakes * Alistair Mees †

September 28, 1991

Abstract

We describe work in progress on using time series data output from dynamical systems to determine information about phase manifolds. Purely from estimates of the probability density of observations, it turns out to be possible in principle to determine the dimension and genus of the manifold. We also show experimental evidence that our methods may be useful for fractal attractors which have nearly integer dimension and are well-approximated by smooth objects such as smooth manifolds with boundary or branched manifolds. Our methods do not use embedding and do not require knowledge of dimensions or choice of time delays or projections.

1 Introduction

Often, data from a dynamical process is only available as a single scalar measurement even although the phase space of the system is high dimensional and may be non-Euclidean. The standard way to handle this problem is to use the embedding theorem [11, 15, 13, 9] and this very powerful result has revolutionised nonlinear data analysis, allowing the calculation of statistics such as fractal dimension [6, 5, 1] as well as the building of dynamical models [3, 4, 2, 7, 8].

A problem that arises whenever embedding is used is how to construct a good embedding. It would be useful to know in advance the dimension of the phase space[1] for the dynamics; other information, such as manifold type, would be useful in construction of qualitative (say, geometrical) models of the action of the dynamics which may sometimes be more informative than black-box quantitative models.

In this paper we use an approach which is independent of embedding and does not require choice of embedding dimensions, lags, projections

*Mathematics Department, The University of Western Australia

†Santa Fe Institute; Center for Nonlinear Science, Los Alamos National Laboratory; on leave from The University of Western Australia

[1] We use the terms "phase space", "phase manifold", "state space" and "state manifold" interchangeably.

and so on. It gives information about the manifold type if the dimension is known, and in principle can give information about the dimension too. The paper is to an extent a report on work in progress, since the proofs are fairly complex as well as new and it is not yet clear whether one can improve the practical usefulness of the approach; consequently, we concentrate here on noise-free data available in reasonable quantities. We do, however, show some evidence from computer experiments that the method works well in the case for which the theorem was originally designed, namely compact smooth manifolds, and may be extensible to other cases, including certain fractal objects.

The long-term aim is to try to find *dynamical signatures*, which allow a (crude) classification of systems in a simple way. The approach is complementary to embedding approaches insofar as it provides separate evidence that the phase space has been correctly identified, and in particular it is complementary to other attempts to identify manifolds using embedding plus triangulation [8].

In the rest of the paper we describe the assumptions we make about the dynamical system and the time series of measurements, and state the basic theorem in the case of compact orientable two-manifolds. Then we discuss some of the background and give a brief plausibility argument for the theorem. Following this are some examples of the theorem in use. Finally, we show some experiments on attractors which are approximately manifolds, although with features that go beyond those in the theorem.

2 Manifolds from data

In this section we outline recent work by Noakes [10] which makes it possible in some circumstances to identify manifold type and dimension from data. The approach is to regard a measurement from a dynamical system as a function of the state, and to assume the function is well-behaved. If we have a trajectory, or a set of trajectories, such that the collection of all the states covers the phase manifold uniformly, then, as is known from embedding theory, well-behaved functions of the states preserve certain information. Surprisingly, some of the information—in particular, the manifold type and dimension—survives even drastic surgery such as replacement of the time series by a density estimator.

A *time series* on a smooth manifold M (without boundary) is a sequence $S = \{x_n : n \geq 1\}$. Let $f : M \to \mathbf{R}$ be a smooth map and write T for the time series $\{y_n \equiv f(x_n) : n \geq 1\}$ on $\mathbf{R}$. Suppose we have a situation where M (and therefore f) and also S is unknown. Can we say anything about the geometry of M by observing T?

Of course, when f is constant we cannot. But most maps are not like that: in fact, an open dense set of smooth maps f is restricted Morse in the following sense.

1. Call $x_i \in M$ *regular* when there is a system (u, v) of local coordinates near x_i in which f takes the form $f(u, v) = u$. When x is not regular

call it a *critical point* of f.

2. Call $x_i \in M$ a *nondegenerate local minimum* when there is a system (u, v) of local coordinates near x_i in which f takes the form

$$f(u, v) = u^2 + v^2.$$

Call $x_i \in M$ a *nondegenerate local maximum* when there is a system (u, v) of local coordinates near x_i in which f takes the form

$$f(u, v) = -u^2 - v^2.$$

3. Say that x_i is a *nondegenerate saddle* when (u, v) can be chosen so that

$$f(u, v) = u^2 - v^2.$$

We call f *restricted Morse* when it is one-to-one on its set C of critical points, and these critical points are either *nondegenerate local maxima* or *nondegenerate local minima* or *nondegenerate saddles.*

Let f be restricted Morse. Then f has only finitely many critical points, and the integer

$$\chi(M) \equiv \#(\text{local minima}) + \#(\text{local maxima}) - \#(\text{saddles}), \qquad (1)$$

called the characteristic, is independent of f and depends only on the geometry of M. If M is orientable (which we assume), $\chi(M)$ determines M up to smooth homeomorphisms. For example, in the case of any manifold M diffeomorphic to a sphere it turns out that $\chi(M) = 2$, while for a torus, $\chi(S^1 \times S^1) = 0$. In fact, for a two-manifold, $1 - \chi/2$ is the number of handles.

If $h : N \to M$ is a smooth homeomorphism, then T might also come from $\tilde{S} \equiv \{\tilde{x}_n = h^{-1}x_n : n \geq 1\}$ by means of the map $\tilde{f} \equiv f \circ h$. So we cannot expect to be able to determine much more about M from the time series than the information given by $\chi(M)$.

This problem, and others, are discussed in [8] in greater detail in the context of manifold triangulation. The present discussion is less ambitious but may be useful in cases where triangulation methods fail for any of a number of reasons; it is also interesting as a method in its own right, since the approach appears to be novel, and may be extensible. One limitation in the present discussion is that S should be more or less uniform with respect to Lebesgue measure; we accept that measures supported by fractal sets are needed in some applications, and we discuss this later. A less essential limitation is that we restrict ourselves here mainly to 2 dimensional manifolds.

Although the time series T does not give much information about M, we are actually going to throw some away. We forget about the ordering of T, so that it becomes an unordered set of real numbers. On the face of it, there is not a lot we can do now except perhaps construct a histogram or other density estimator for T. For this paper, we are only going to look at histograms and a closely related estimator.

Suppose that the x_n are realisations of a random variable X described by a never-zero smooth density f on M with respect to a smooth never-zero area form μ. Then $y_n = f(x_n)$ is representative of $Y \equiv f(X)$. But $\hat{g}$ is an estimate for a probability density function g for Y. The following result is nontrivial and is proved in [10] using techniques from differential geometry.

Theorem 1 *Let $f : M \to \mathbf{R}$ be restricted Morse. There is a smooth density g for $Y \equiv f(X)$ with the following properties:*

1. *g is defined over $f(M) - f(C)$;*
2. *if z_0 is the image of a point of local minimum of f then z_0 is a* left cliff *of g, namely*
$$\lim_{z \to z_0^+} g(z) > \lim_{z \to z_0^-} g(z),$$
and if z_0 is the image of a point of local maximum of f then z_0 is a right cliff *of g, namely*
$$\lim_{z \to z_0^+} g(z) < \lim_{z \to z_0^-} g(z);$$
3. *if z_0 is the image of a saddle of f then z_0 is a* splinter *of g, namely*
$$g(z) = -O(\ln|z - z_0|)$$
for z near z_0.

An idea of why the result holds can be got from thinking about how densities project. Near a point $x_{(0)}$ of local minimum our restricted Morse function f takes the form $f(u, v) = f(x_{(0)}) + u^2 + v^2$ where u, v are local coordinates in a neighbourhood of $x_{(0)}$. Write $r^2 = u^2 + v^2$. When $Y \geq 0$ the infinitesimal contribution to the probability of $Y \equiv f(X)$ from this neighbourhood is more or less $2\pi r dr = \pi d(r^2) = \pi dY$ and so the contribution to the density is π. On the other hand, when $Y < 0$ the neighbourhood contributes nothing to the probability of Y. So we have π on the right and 0 on the left, added to which there may be a smooth contribution from regions outside the neighbourhood. The result is a cliff. The argument generalises, of course: for example, a three-manifold gets a contribution of $4\pi r^2 dr = 2\pi r d(r^2) = 2\pi Y^{1/2} dY$, and the cliff is replaced by the positive part of a square root function.

So if we plot $\hat{g}$ the features characteristic of local maxima and minima and of saddles may stand out. By counting their numbers we should be able to estimate $\chi(M)$. Code for finding a standard equal-width bin histogram is readily available, or is easy to write. The time required for the calculation is, of course, very short. Figure 1 shows an example for a torus, where the upper part of the picture is a two dimensional projection of a torus embedded in three dimensions and the lower part is the one dimensional projection onto the axis shown. We see cliffs corresponding to "outside curves" from the viewpoint implied by the upper picture, and splinters corresponding to "inside curves". The numbers of cliffs and

splinters are the same, so the formula gives $\chi = 0$ as we would expect. Note that one way in which genericity is important is that we do not want a cliff and a splinter (for example) to coincide in the one dimensional projection.

There are analogous, but less informative, procedures for higher dimensional manifolds. The reason they are less informative is that the signatures of extreme points and saddles become less pronounced: for example, we indicated above that for a three-manifold a cliff is replaced by a square root function.

3 Applications

We first describe two examples of direct use of the theorem; for more details and other examples, see [10]. Then we consider how to better estimate the features like cliffs and splinters that we are looking for, and apply a modified estimator to a quasiperiodic signal to reveal the underlying torus.

3.1 Example

We distribute 100,000 points (x_1, x_2, x_3, x_4) uniformly over the torus $S^1 \times S^1$ in $\mathbf{R}^4$, by setting

$$(x_1, x_2, x_3, x_4) = (\cos\theta, \sin\theta, \cos\phi, \sin\phi)$$

for θ and ϕ distributed independently on $(0, 2\pi)$. We define the observation function f by

$$f(x_1, x_2, x_3, x_4) = (x_1 - 1.8)^2 + (x_3 - 3.7)^2.$$

The critical points of f can be calculated directly and occur at

(1,0,1,0)	(minimum)	value 7.93
(-1,0,-1,0)	(maximum)	value 29.93
(1,0,-1,0)	(saddle)	value 22.73
(-1,0,1,0)	(saddle)	value 15.13.

A histogram of the values of $y = f(x_1, x_2, x_3, x_4)$ is shown in Figure 2. There are two cliffs and two splinters, where the Theorem says they should be. This is also in agreement with formula (1) since $\chi(S^1 \times S^1) = 0$. Figure 3 shows that the features are still evident with only 5,000 data points.

3.2 Example

We take 100,000 points distributed uniformly over S^2 embedded in $\mathbf{R}^3$, with $f(x_1, x_2, x_3) = (x_1 + 3)(x_2 + 1)(x_3 + 2)$. We would have guessed $M \approx S^2$ from formula (1) and the histogram in Figure 4, which has two cliffs and no splinters, implying $\chi(S^2) = 2$.

3.3 Other methods of density estimation

A more classically-based approach to estimating the phase manifold M, used in [8], is to use the ordering of T to define an embedding of M in Euclidean space, and then triangulate the resulting cloud of points. This might lead to enhanced estimates, in that smaller samples might be required to estimate $\chi(M)$ accurately, but it may also require a lot of technique to implement successfully, particularly if the data is corrupted by noise or is inaccurate for other reasons. Although we have not discussed the effects of noise on the approach being described here, it is reasonable to expect that small noise on the data should not greatly affect the appearance of the histogram: the main problem will be the blurring of important features, with the risk that, say, a quadratic maximum in the density function becomes indistinguishable from a splinter.

Although we have used large numbers of points in the examples so far, cleverer density estimation techniques could perhaps be used to reduce the size of time series required, at least in the low-noise case. We have not, however, had much success using standard smoothing of histograms; nor would we expect to have much success using smooth kernel approximation, since both of these techniques are intended for estimating smooth densities and obscure precisely the features we wish to find.

A technique which may be better adapted to the present problem is to try to fit the density more carefully in regions where there are many data points. The following simple method first estimates the distribution function (i.e., the integral $P(y)$ of the density). To do so it sorts the data $\{y_i\}$ into increasing order, giving a series $\{s_i\}$, which gives points $(s_i, i/n)$. A crude piecewise-linear (discontinuous) estimator of P is obtained by fitting straight line segments to subsets of points $(s_i, i/n) : \ i_0 \leq i \leq i_1$, for various values of i_0 and i_1. The slopes of the lines are then estimates of the density. We have found this useful with subsets ranging in size from 50 to 1000, depending on the number of data points available.

3.4 Example

A segment of the function

$$y(t) = \cos(t) + \sin(\omega t)$$

(where $\omega = \exp(1)$) is shown in Figure 5. Take a sample of 40,000 points (sampled at time intervals of 0.4) from $y(t)$ and apply this approach: the result is in Figure 6. We do not need such a huge sample, however: Figure 7 shows that the features are still apparent in the estimate using this method with only 1,000 points and subsets of size 40 (i.e., 25 bins).

The technique we have used here can be regarded as a variable-width binning method, but it is sensitive to noise and, when there is comparatively little data, to subset size; it should probably be used in conjunction with standard histograms. It is certainly worthwhile trying different numbers of bins: for example, with the torus the splinters and cliffs stand out with bins containing very small numbers of points (down to 2 or so) but

there are many spurious smaller peaks, while with too many points per bin the splinters are broadened to the extent that they become insignificant.

4 Application to non-manifolds

Encouraged by our success with two-manifolds, we now investigate empirically how much further this kind of analysis can be pushed. Our main interest is in dynamical systems where M is replaced by a fractal set which is "thin" in that its dimension is approximately an integer, and that it is well-approximated by a manifold, possibly with branches or boundaries, and possibly non-orientable. (The analysis given earlier can be extended to such more general manifolds, but our interest here is in the fractal objects.)

4.1 Example

We take 9,000 points from the Rossler attractor [12] and estimate the density. The resulting graph in Figure 8 has many of the features of the previous examples, especially the cliffs at either end which are characteristic of dimension (approximately) 2. Note also the sharp points which resemble the splinters observed in Figure 1. The approximating surface is made by gluing a Mobius band, which is a non-orientable manifold with boundary, to an annulus, which is an orientable manifold with boundary.

4.2 Example

When we do the same thing with 9,000 points from the Lorenz attractor [14] we obtain Figure 9. Similar comments apply, except that the cliffs are less pronounced: we need a lot more data to see what is really happening at the edges, and in fact we expect to see fractal structure, rather than actual cliffs. Fractal structure at the edges is one of the features which will show up in a better density estimator: there are already indications in Figure 9, and a better estimator might also show such structure in Figure 8. We are currently investigating whether we can estimate dimension from such fractal structure.

4.3 Example

To convince ourselves that we are not doing something trivial, we do the same thing with times between geiger counter detections of radioactive emissions from decay of radioactive cobalt. Figure 10 certainly does not look like a histogram of data collected from a time series whose phase-manifold is two-dimensional, and of course it is not: the data should consist of realisations of independent identically exponentially distributed random variables, which the graph does not contradict.

5 Conclusions

It is a little surprising that information about the nature of the system's state space is available directly from density estimators of a time series or other sample. With the tools we have at present, practical use is limited, and the density approach can best be regarded as complementary to others, but further developments may give rise to a method of increased scope and robustness.

Acknowledgements

AIM thanks the University of Western Australia, the Santa Fe Institute and Los Alamos National Laboratory for support. This research was partially funded by an ARC grant.

References

[1] Albano, A. M., A. I. Mees, G. C. deGuzman & P. E. Rapp, "Data requirements for reliable estimation of correlation dimensions", eds. Degn, H., A. V. Holden & L. F. Olsen, *Chaos in biological systems*, Plenum, New York (1987), pp. 207-220.

[2] Casdagli, M., "Nonlinear prediction of chaotic time series", *Physica D*, vol. 35 no. 3, (1989): 335-356.

[3] Eckmann, J.-P. & D. Ruelle, "Ergodic theory of chaos and strange attractors", *Reviews of Modern Physics*, vol. 57 no. 3, (1985): 617-656.

[4] Farmer, J. D. & J. J. Sidorowich, "Predicting chaotic time series", *Physical Review Letters*, vol. 59 no. 8, (1987): 845-848.

[5] Farmer, J. D., E. Ott & J. A. Yorke, "The dimension of chaotic attractors", *Physica D*, vol. 7D, (1983): 153-180.

[6] Grassberger, P. & I. Procaccia, "Measuring the strangeness of strange attractors", *Physica D*, vol. 9, (1983): 189-208.

[7] Mees, A. I., "Modelling Complex Systems", eds. Vincent, T., A. I. Mees & L. S. Jennings, *Dynamics of Complex Interconnected Biological Systems*, Birkhauser, Boston (1990), pp. 104-124.

[8] Mees, A. I., "Dynamical systems and tesselations: detecting determinism in data", *International Journal of Bifurcation and Chaos in Applied Science and Engineering*, vol. 1 no. 4, (1991): in press.

[9] Noakes, L. "The Takens embedding theorem", *International Journal of Bifurcation and Chaos*, in press (1991).

[10] Noakes, L. In preparation.

[11] Packard, N. H., J. P. Crutchfield, J. D. Farmer & R. S. Shaw, "Geometry from a Time Series", *Physical Review Letters*, vol. 45 no. 9, (1980): 712-716.

[12] Rossler, O. E., "An equation for continuous chaos.", *Physics Letters* vol. 57A no. 5, (1976): 397-398.

[13] Sauer, T., J.A. Yorke & M. Casdagli, "Embedology", *Comm. Math. Phys.*, under consideration, 1991.

[14] Sparrow, C. T., *The Lorenz Equations: Bifurcations, Chaos and Strange Attractors,* New York: Springer, 1982.

[15] Takens, F., "Detecting strange attractors in turbulence", *Lecture Notes in Mathematics,* vol. 898, New York: Springer, 1981.

Figure 1: A possible density for a 2-torus embedded in $\mathbf{R}^3$. Cliffs are marked "c" and splinters are marked "s". There are as many cliffs as splinters, implying that $\chi(S^1 \times S^1) = 0$.

Figure 2: Density plot (100 bins) for 100,000 samples from real-valued observations of a uniform distribution on a 2-torus embedded in $\mathbf{R}^4$. There are 2 cliffs and 2 splinters.

Figure 3: Density plot (100 bins) for 5,000 samples from the torus as in Figure 2. The cliffs and splinters are still visible.

Figure 4: Density plot (100 bins) for 100,000 samples from a uniform distribution on a 2-sphere embedded in $\mathbf{R}^3$. The observation function is $(x+3)(y+1)(z+2)$. There are 2 cliffs and no splinters.

Figure 5: A quasiperiodic waveform, created by a dynamical system on a 2-torus.

Figure 6: Modified density estimating algorithm applied to 40,000 data values from the waveform of Figure 5. The phase space is identified as a torus by the 2 cliffs and 2 splinters.

Figure 7: The identifying features of the 2-torus are still present in the density estimate from the modified algorithm, even with only 1,000 points and 25 bins.

Figure 8: Modified density estimate (100 bins) for 9,000 samples from the Rossler attractor. There appear to be cliffs and perhaps splinters.

Figure 9: Modified density estimate (100 bins) for 9,000 samples from the Lorenz attractor.

Figure 10: Modified density estimate (100 bins) for 21,000 intervals between detections of emissions from radioactive cobalt.

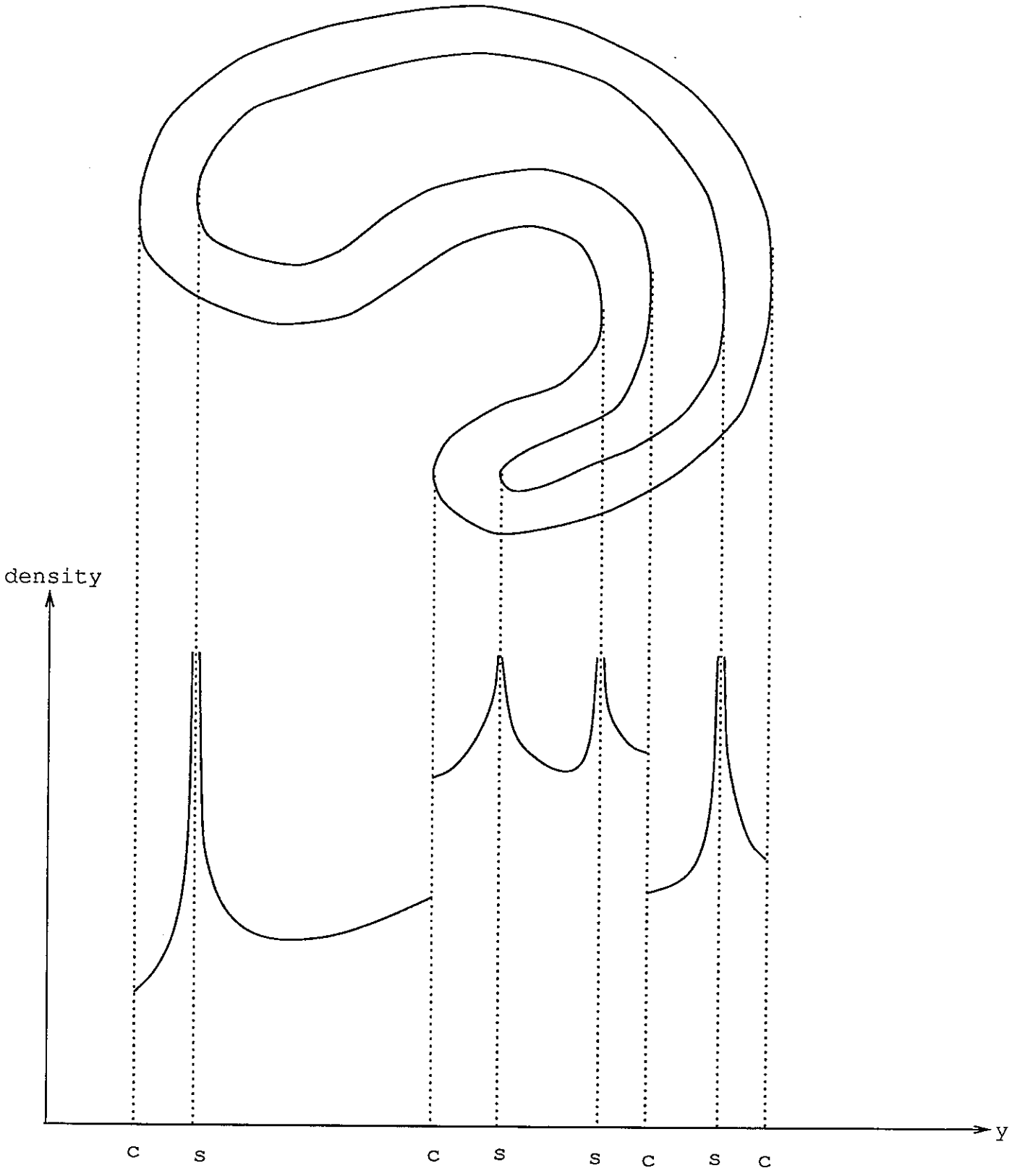

Nuales - Moss Fig 1

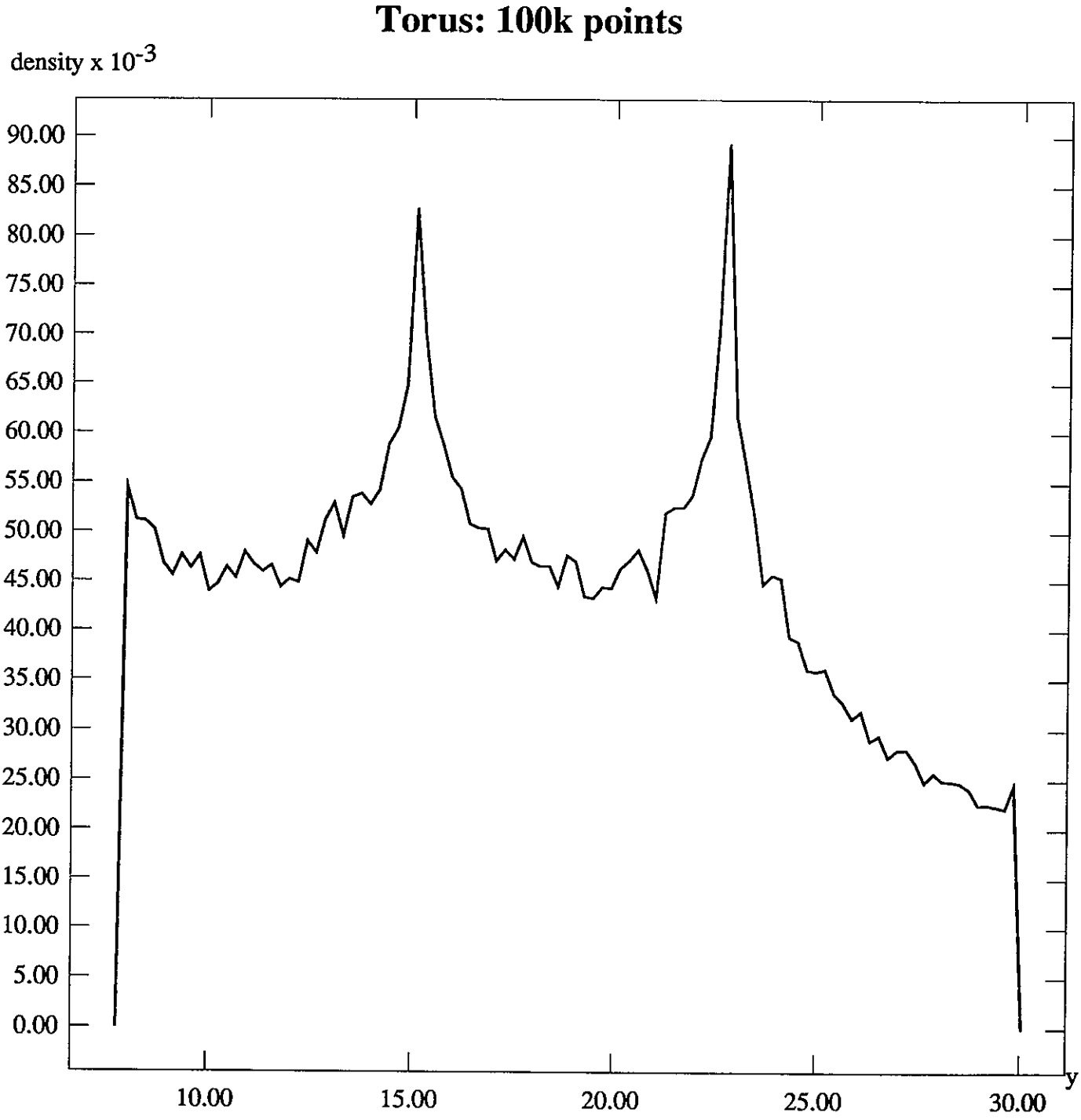

Meakin-Moss Fig 2

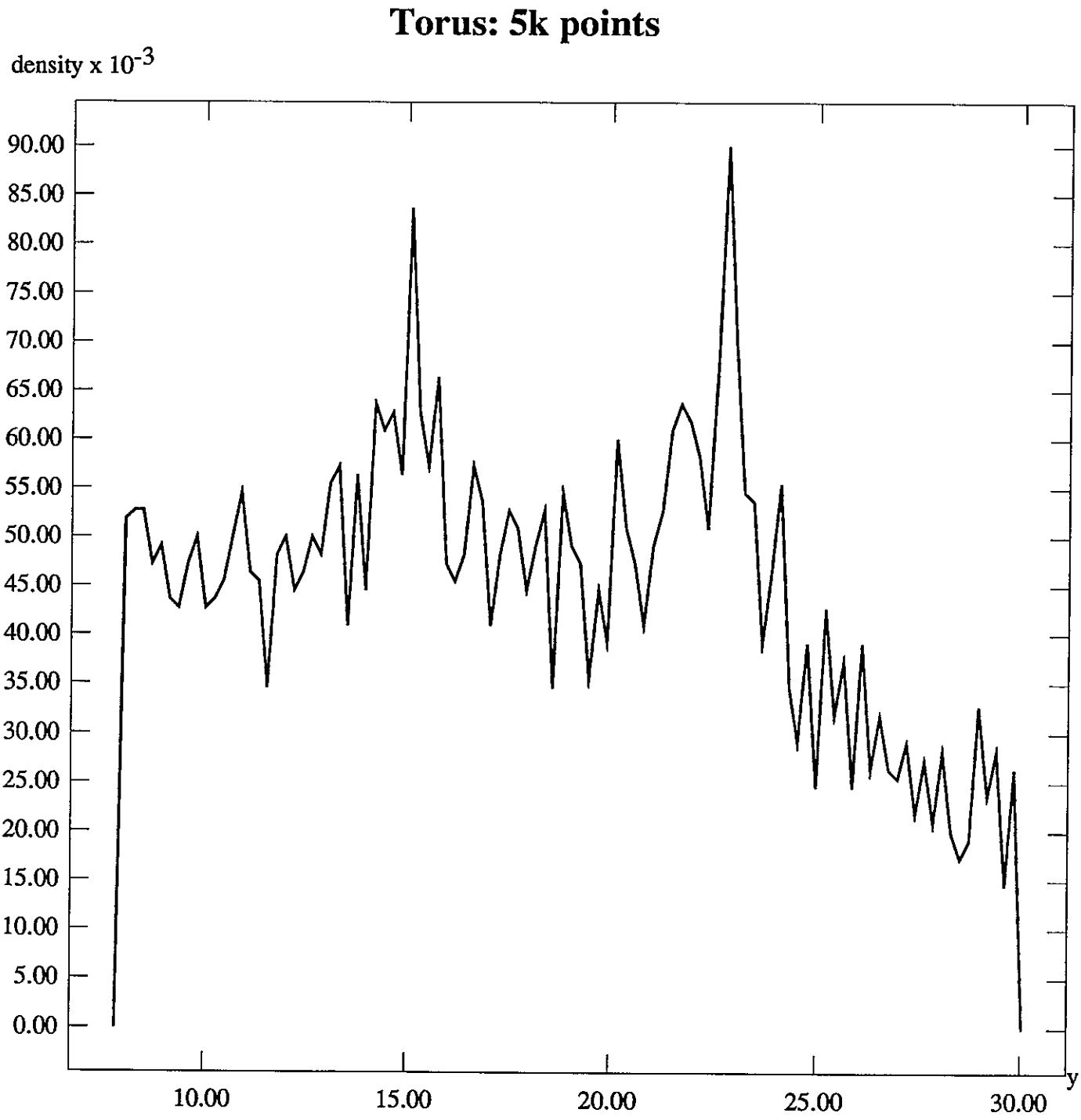

Nowbar - Mass Fig 3

Sphere: 100k points

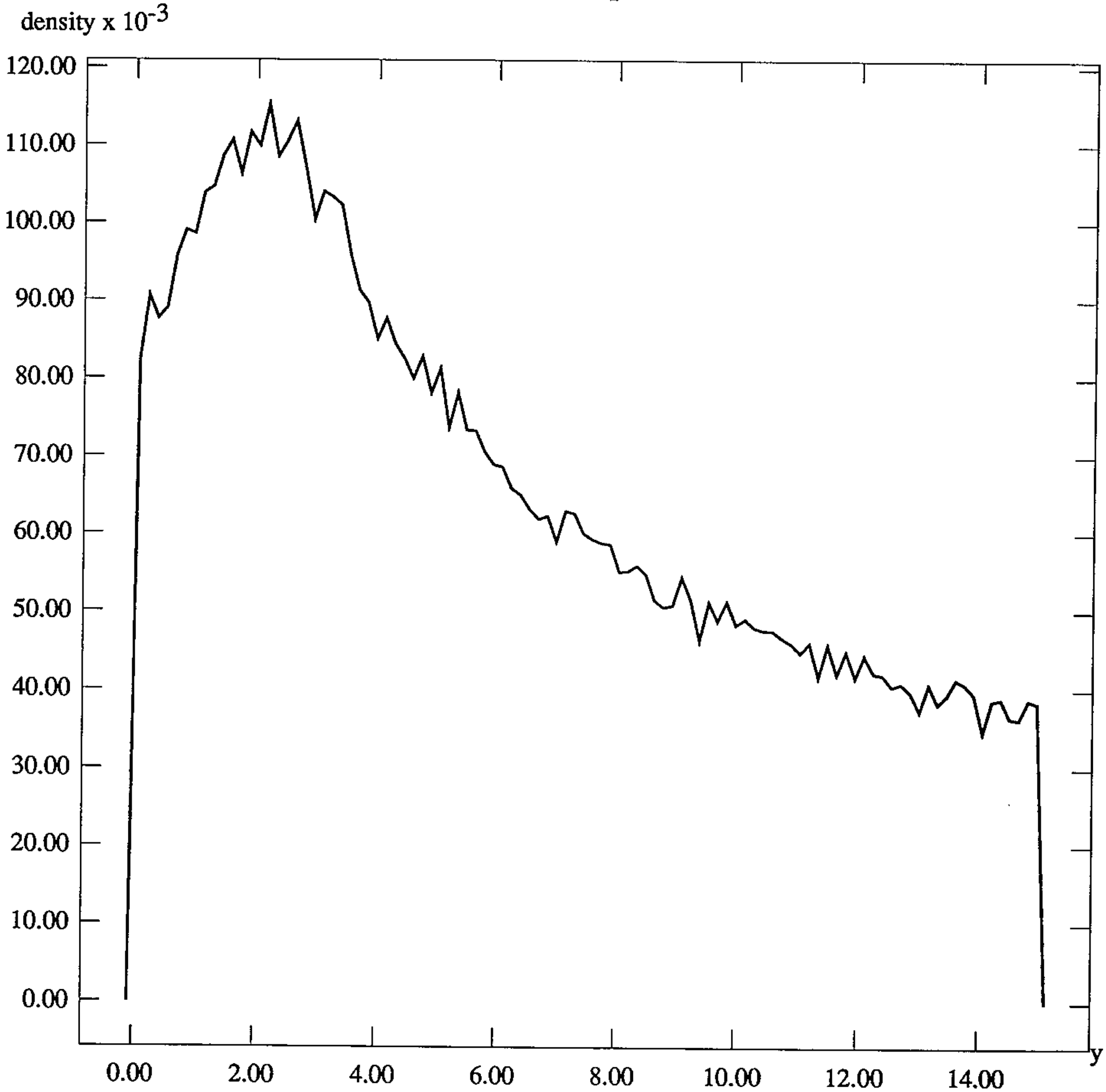

Norden Mells Fig 4

Quasiperiodic signal

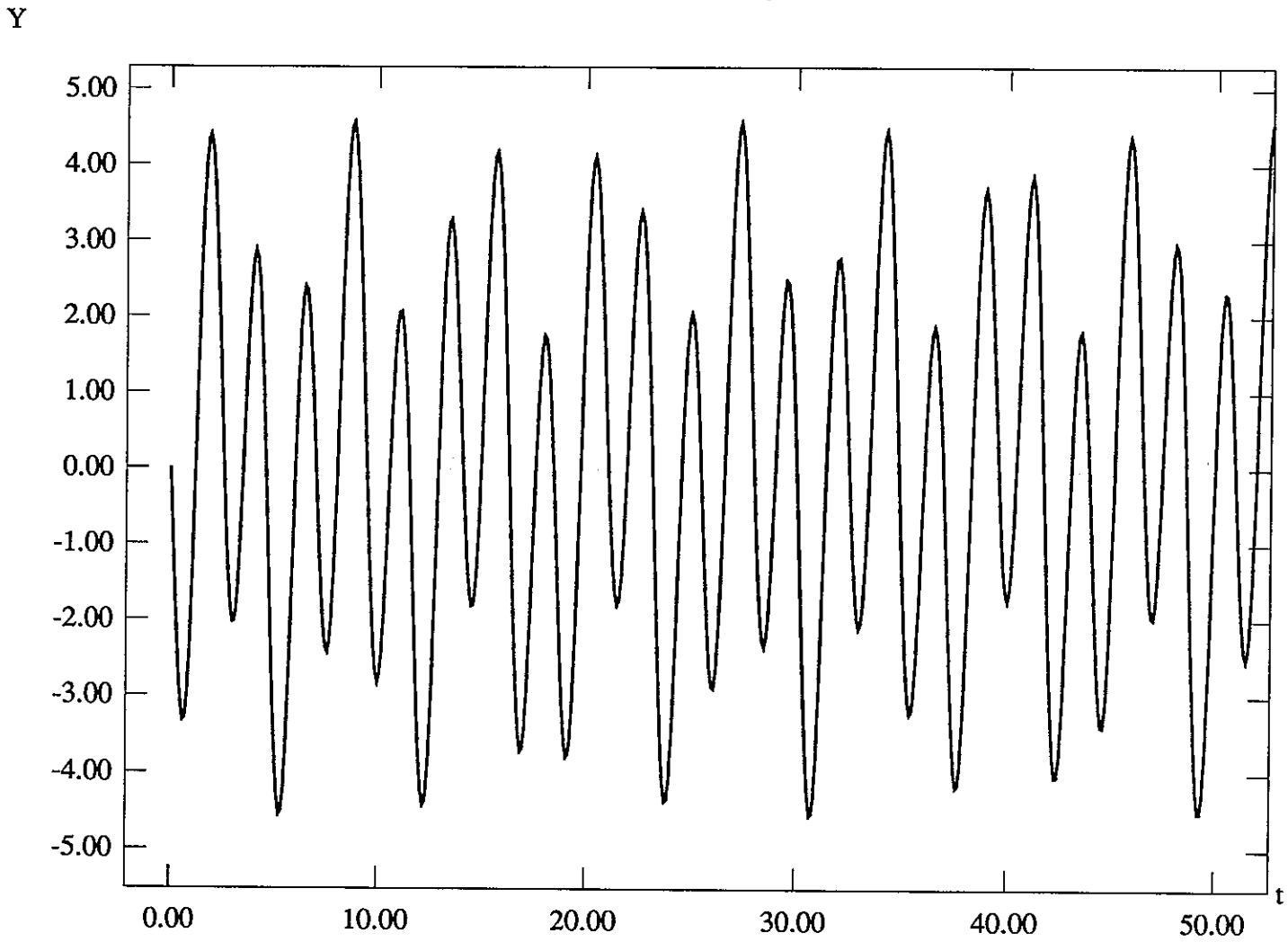

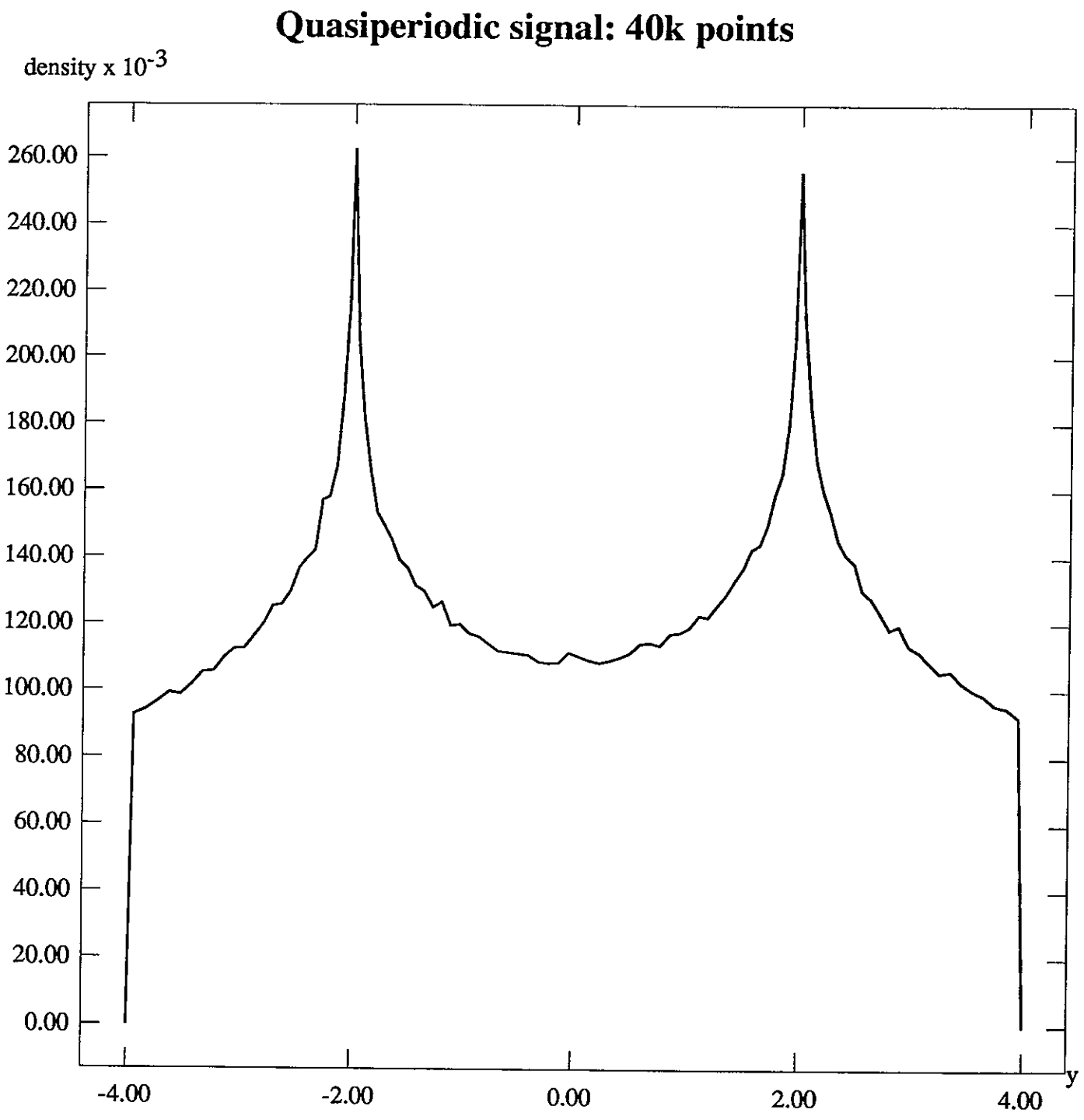

Nordes - Moss Fig 6

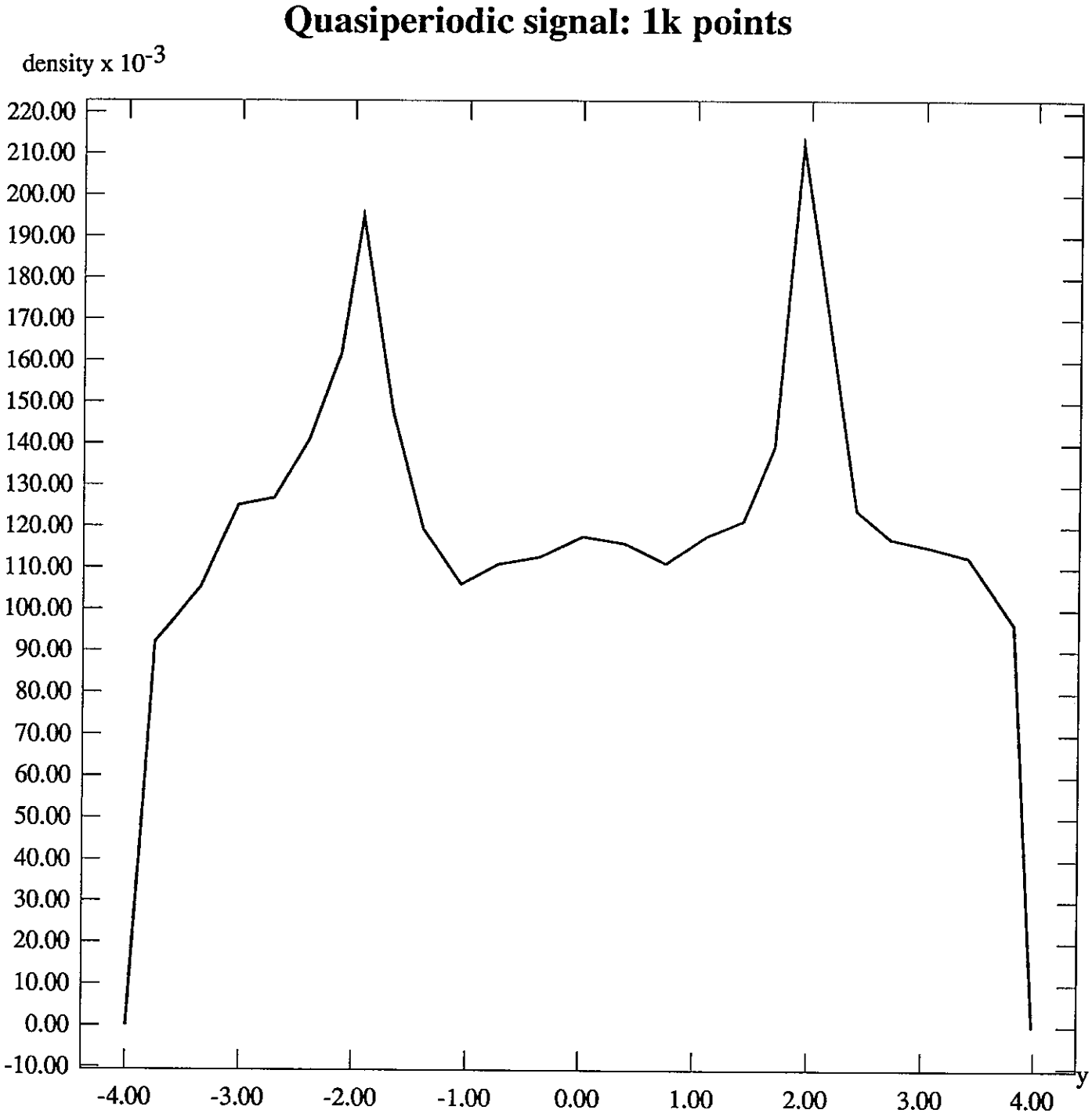

Noah's Mom Fig 1

Rossler: 9k points

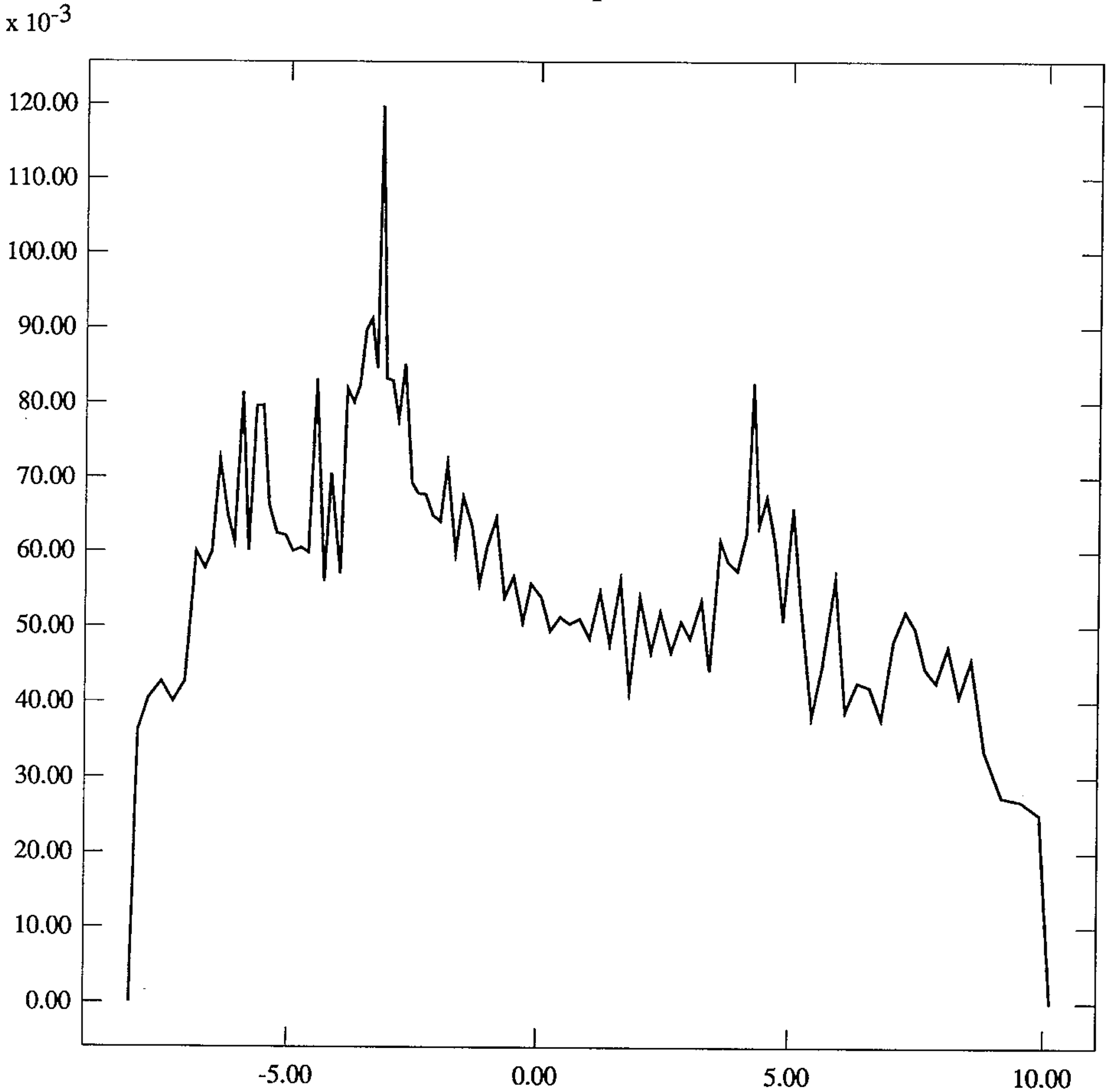

[illegible] Fig 8

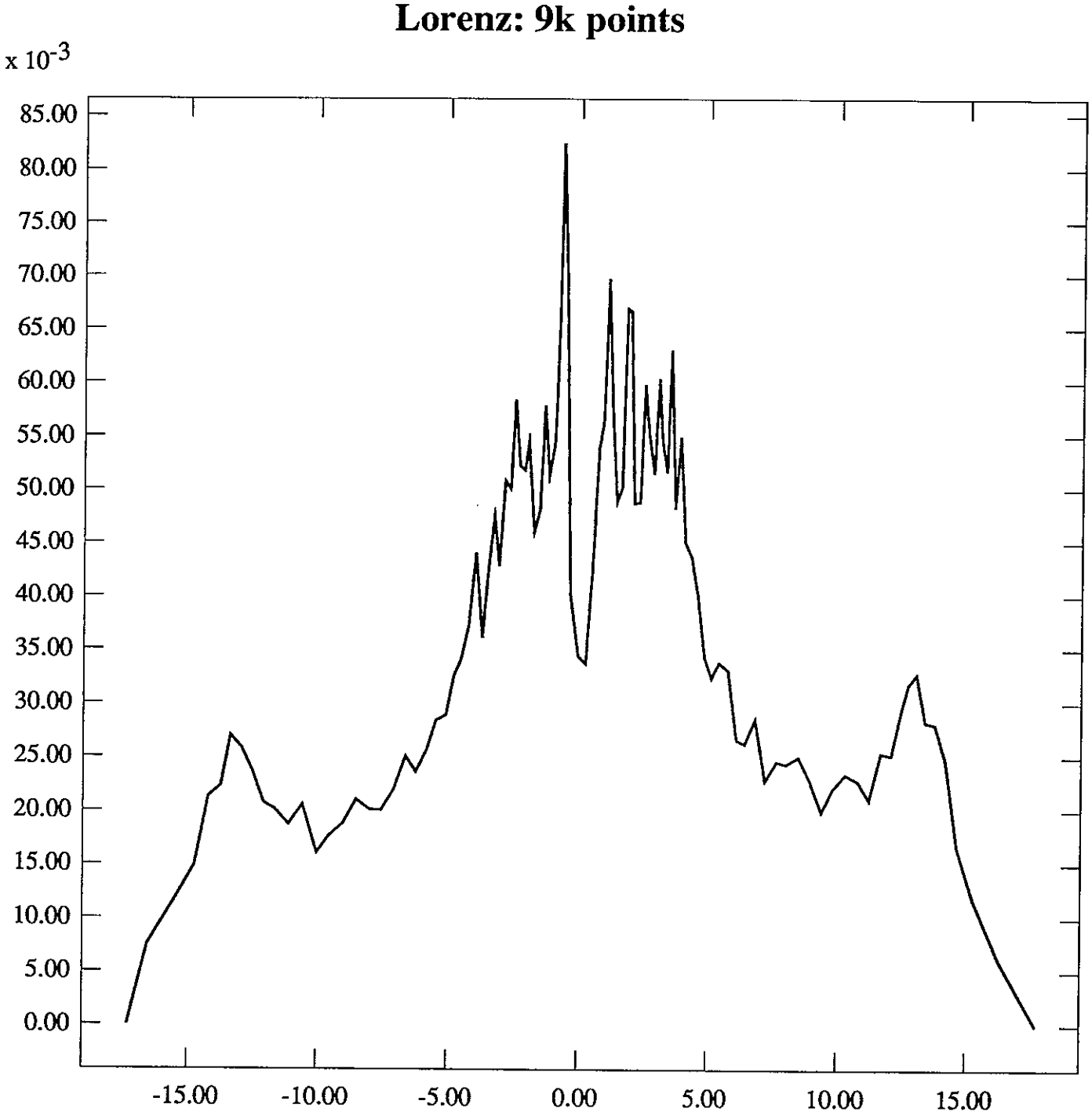
Lorenz: 9k points
x 10-3
85.00
80.00
75.00
70.00
65.00
60.00
55.00
50.00
45.00
40.00
35.00
30.00
25.00
20.00
15.00
10.00
5.00
0.00
-15.00
-10.00
-5.00
0.00
5.00
10.00
15.00

Radioactive decay: 21k points

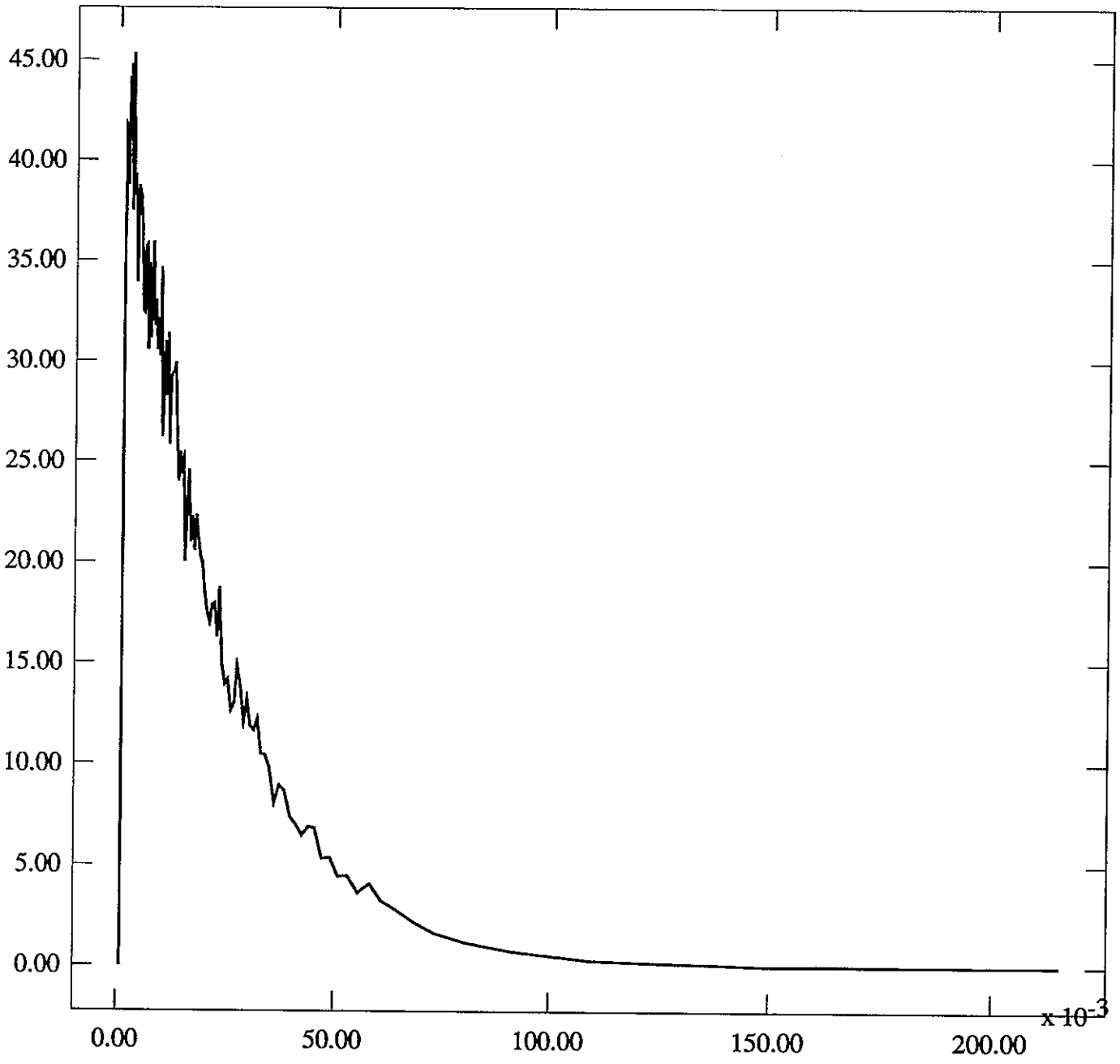

Nuclear - Nucl Fig 10